MIT Libraries | DSpace@MIT

MIT Open Access Articles

# *Sequence-Dependent Variation in the Reactivity of 8-Oxo-7,8-dihydro-2#-deoxyguanosine toward Oxidation*

The MIT Faculty has made this article openly available. ***Please share*** how this access benefits you. Your story matters.

**Citation:** Lim, Kok Seong, Koli Taghizadeh, John S. Wishnok, I. Ramesh Babu, Vladimir Shafirovich, Nicholas E. Geacintov, and Peter C. Dedon. "Sequence-Dependent Variation in the Reactivity of 8-Oxo-7,8-Dihydro-2#-Deoxyguanosine Toward Oxidation." Chemical Research in Toxicology 25, no. 2 (February 20, 2012): 366–373.

**As Published:** http://dx.doi.org/10.1021/tx200422g

**Publisher:** American Chemical Society

**Persistent URL:** http://hdl.handle.net/1721.1/88712

**Version:** Author's final manuscript: final author's manuscript post peer review, without publisher's formatting or copy editing

**Terms of Use:** Article is made available in accordance with the publisher's policy and may be subject to US copyright law. Please refer to the publisher's site for terms of use.

Massachusetts Institute of Technology

NIH Public Access
Author Manuscript
*Chem Res Toxicol*. Author manuscript; available in PMC 2013 February 20.

Published in final edited form as:
*Chem Res Toxicol*. 2012 February 20; 25(2): 366–373. doi:10.1021/tx200422g.

# Sequence-dependent Variation in the Reactivity of 8-Oxo-7,8-dihydro-2'-deoxyguanosine toward Oxidation

**Kok Seong Lim**[†,*], **Koli Taghizadeh**[‡], **John S. Wishnok**[†,‡], **I. Ramesh Babu**[‡], **Vladimir Shafirovich**[§], **Nicholas E. Geacintov**[§], and **Peter C. Dedon**[†,‡,*]

[†]Department of Biological Engineering, Massachusetts Institute of Technology, Cambridge, Massachusetts

[‡]Center for Environmental Health Sciences, Massachusetts Institute of Technology, Cambridge, Massachusetts

[§]Department of Chemistry, New York University, New York, New York

## Abstract

The goal of this study was to define the effect of DNA sequence on the reactivity of 8-oxo-7,8-dihydro-2'-deoxyguanosine (8-oxodG) toward oxidation. To this end, we developed a quadrupole/time-of-flight (QTOF) mass spectrometric method to quantify the reactivity of site-specifically modified oligodeoxyribonucleotides with two model oxidants: nitrosoperoxycarbonate ($ONOOCO^-_2$), a chemical mediator of inflammation, and photoactivated riboflavin, a classical one-electron oxidant widely studied in mutagenesis and charge transport in DNA. In contrast to previous observations with guanine (Margolin, Y., et al., *Nat. Chem. Biol. 2*, 365, 2006), sequence context did not affect the reactivity of $ONOOCO_2^-$ with 8-oxodG, but photosensitized riboflavin showed a strong sequence preference in its reactivity with the following order (8-oxodG = O): COA ≈ AOG > GOG ≥ COT > TOC > AOC. That the COA context was the most reactive was unexpected and suggests a new sequence context where mutation hotspots might occur. These results point to both sequence- and agent-specific effects on 8-oxodG oxidation.

### Keywords

DNA damage; mass spectrometry; oxidative stress; reactive nitrogen species; reactive oxygen species; riboflavin; DNA sequence; oligodeoxyribonucleotide

## INTRODUCTION

The sequence dependence of DNA oxidation was first suggested in the 1980s,[1] and has since been the subject of intense study.[2,3] Ito and Saito provided early experimental evidence showing that photooxidation of the DNA duplex occurred preferentially at guanine (G) nucleobases located at the 5' end of runs of G.[4–6] They proposed that the key to this selectivity lay in the sequence dependence of the G oxidation potential, so, using *ab initio* approaches, they calculated the ionization potentials (IP) for G in all 16 three-nucleotide sequence contexts, values later refined by Siebbeles and coworkers.[7] A comparison of IP to reactivity toward oxidation by photoactivated riboflavin, a type I photosensitizer that causes one-electron oxidation,[8] revealed the expected inverse correlation.[9] More recently, we

[*]Address all correspondence to: Peter C. Dedon, pcdedon@mit.edu. Kok Seong Lim, kslim@mit.edu.

**SUPPORTING INFORMATION AVAILABLE** The supporting information includes two supplementary tables and three supplementary figures. This material is available free of charge via internet at http://pubs.acs.org.

NIH-PA Author Manuscript
NIH-PA Author Manuscript
NIH-PA Author Manuscript

NIH-PA Author Manuscript

NIH-PA Author Manuscript

NIH-PA Author Manuscript

observed that the sequence-dependence of G oxidation was oxidant-specific, with $ONOOCO_2^-$ reacting preferentially with CGC, AGC, and TGC, in which G has the highest IP, in direct contrast to riboflavin-mediated photooxidation.[10,11] $ONOOCO_2^-$ is the $CO_2$ conjugate of peroxynitrite ($ONOO^-$) that arises in reactions of macrophage-derived nitric oxide (NO) with superoxide ($O_2^{\bullet-}$). It decomposes rapidly into $^{\bullet}NO_2$ and $CO_3^{\bullet-}$, which are weak and strong oxidants, respectively. While $CO_3^{\bullet-}$ is capable of oxidizing G, both $^{\bullet}NO_2$ and $CO_3^{\bullet-}$ are capable of oxidizing 8-oxo-7,8-dihydro-2'-deoxyguanosine (8-oxodG),[12] a major G oxidation product that is orders-of-magnitude more susceptible to oxidation than G due to its lower reduction potential.[13–16] These observations raise the question of the role of sequence context in the oxidation of 8-oxodG. While 8-oxodG was shown to be more reactive when located 5' rather than 3' to a G[17] presumably due to a lower sequence-dependent IP,[13] the broader question of sequence context effects has not been addressed. Here we compare the reactivity of 8-oxodG toward oxidation by $ONOOCO_2^-$ and riboflavin-mediated photooxidation in sequence contexts spanning the range of guanine reactivities and sequence-dependent G IP values.

## EXPERIMENTAL PROCEDURES

### Materials

All chemicals and reagents were of the highest purity available and were used without further purification. Ammonium acetate, sodium chloride and tris(hydroxymethyl)aminomethane were purchased from American Bioanalytical (Natick, MA); EDTA, potassium phosphate, sodium bicarbonate from Mallinckrodt (Paris, KY); acetonitrile from EMD Chemicals (Gibbstown, NJ); peroxynitrite from Cayman Chemical (Ann Arbor, MI; peroxynitrite concentration was determined spectrophotometrically in 0.3 M NaOH with $A_{302}$ = 1670 $M^{-1}cm^{-1}$); riboflavin from Sigma (St. Louis, MO). Deionized water was purified with a Milli-Q system (Millipore Corporation, Bedford, MA) and autoclaved prior to use in all experiments. The oligodeoxyribonucleotides used in these experiments were purchased from the Midland Certified Reagent Company, Inc. (Midland, TX) and their sequences are shown in Table 1. Double-stranded oligodeoxyribonucleotides were prepared by mixing the 8-oxodG-containing strands (8-oxodG oligodeoxyribonucleotide) with a 15% excess of the complementary strand in 10 mM Tris buffer (pH 8), 50 mM NaCl and 1 mM EDTA, heating the mixture to 95 °C for 5 min and then cooling the mixture to 4 °C at a rate of 1 °C/min.

### Determination of oligodeoxyribonucleotide melting temperatures

To ensure that oligodeoxyribonucleotide substrates were fully double-stranded under the experimental conditions (4–18 °C), we determined their melting temperatures by two different approaches: real-time PCR and circular dichroism. In both cases, solutions of 20 μM duplex oligodeoxyribonucleotides were prepared in 150 mM sodium phosphate buffer (pH 7.4) containing 25 mM sodium bicarbonate to mimic the oxidation reaction conditions described below. Melting curves based on real-time PCR dissociation analysis were performed using the 7900HT Fast Real-Time PCR system (Applied Biosystems, Carlsbad, CA), with fluorescence recorded continuously from 15 to 95 °C at a ramp rate of about 2 °C/min. Melting curves obtained by circular dichroism (CD) were recorded using a CD spectrometer Model 410 (Aviv Biomedical, Lakewood, NJ), with 1-mm path length quartz cuvette, at 250 nm from 10 to 90 °C in 2 °C increments and 6 s recording time. The melting temperatures were calculated from these data using Origin 8.0 software (OriginLab, Northampton, MA).

NIH-PA Author Manuscript

NIH-PA Author Manuscript

NIH-PA Author Manuscript

### Treatment of oligodeoxyribonucleotides with oxidants

Oxidation of double-stranded oligodeoxyribonucleotides was performed with 20 μM oligodeoxyribonucleotide in 150 mM potassium phosphate buffer and 25 mM sodium bicarbonate (final pH 7.4) using a range of oxidant concentrations as described in the text. For $ONOOCO_2^-$ treatment, a droplet of peroxynitrite ($ONOO^-$) was added to the sidewall of a tube containing a solution of the oligodeoxyribonucleotide solution, along with another droplet of equal volume of 0.3 M HCl to neutralize the NaOH. Following rapid mixing by vortexing, HCl neutralized the basic $ONOO^-$ solution and $ONOOCO_2^-$ was generated by rapid, direct reaction of $ONOO^-$ with $CO_2$. The sample was incubated for 30 min at 18 °C. Riboflavin-mediated photooxidation was achieved by adding riboflavin to the oligodeoxyribonucleotide solution and exposing the mixture to ultraviolet A light (350 nm) using a Rayonet reactor (Southern New England Ultraviolet Company, Branford, CT) for 20 min at 4 °C. After both treatments, an equimolar quantity of internal standard (5'-GATCTCGATC-3') was added to the reaction mixture to account for variations in the volume injected onto the HPLC column. The treated oligodeoxyribonucleotides were then desalted prior to analysis by liquid chromatography-coupled mass spectrometry.

### High performance liquid chromatography-coupled mass spectrometric (LC-MS) analyses of oligodeoxyribonucleotides

HPLC was performed on an Agilent series 1200 instrument (Agilent Technologies, Santa Clara, CA) consisting of a binary pump, a solvent degasser, a thermostatted column compartment and an autosampler. Oligodeoxyribonucleotide separation was achieved using reversed-phase HPLC with a Hypersil GOLD aQ C18 column (150 mm × 2.1 mm, 3 μm particle; Thermo Scientific, Waltham, MA) and a guard column (10 mm × 2.1 mm, 3 μm particle). The mobile phase flow rate was 250 μL/min and the column temperature was maintained at 25 °C. The solvent system was 10 mM ammonium acetate (A) and acetonitrile (B), with the elution started isocratically at 3% B for 2 min, followed by a linear gradient from 3 to 12% B over 9 min and further to 40% B over 2.5 min, and finally the column was re-equilibrated at 3% B for 10 min.

Identification and quantification of oligodeoxyribonucleotides was accomplished by coupling the HPLC to an Agilent 6510 quadrupole time-of-flight (QTOF) mass spectrometer equipped with an electrospray ionization (ESI) source operated in negative ion mode. Operating parameters were as follows: ESI capillary voltage, 4000 V; gas temperature, 350 °C; drying gas flow, 10 L/min; nebulizer pressure, 50 psi; fragmentor voltage, 200 V; *m/z* scan range, 900–1200. The collision-induced dissociation (CID) fragmentation of an oligodeoxyribonucleotide was performed under the same conditions with a *m/z* scan range of 300–1600, with fragmentation patterns predicted using Mongo Oligo Mass Calculator (v2.06) (http://library.med.utah.edu/ masspec/mongo.htm). In some cases, oligodeoxyribonucleotide quantification was achieved using an Agilent 6410 triple quadrupole (QQQ) system equipped with an ESI source operated in the negative ion mode. Operating parameters were as follows: ESI capillary voltage, 4000 V; gas temperature, 330 °C; drying gas flow, 10 L/min; nebulizer pressure, 20 psi; fragmentor voltage, 150 V. Table S1 shows the multiple reaction monitoring (MRM) transitions used in these studies. Agilent Mass Hunter workstation software version B.03.01 was used for data processing.

### Quantification of 8-oxodG nucleoside using liquid chromatography-coupled triple quadrupole mass spectrometry

The treated oligodeoxyribonucleotide samples were enzymatically hydrolyzed to 2'-deoxynucleosides as described previously.[18] The enzymes were then removed by filtration (Nanosep 10K centrifugal device; Pall Corporation, Port Washington, NY). An aliquot of the sample was analyzed by HPLC-ESI-MS/MS using an Agilent 1100 series HPLC system

NIH-PA Author Manuscript

NIH-PA Author Manuscript

NIH-PA Author Manuscript

interfaced with an Agilent 6410 triple quadrupole mass spectrometer. Nucleoside separation was achieved using reversed-phase HPLC with a Hypersil GOLD aQ C18 column (150 mm × 2.1 mm, 3 μm particle; Thermo Scientific, Waltham, MA) and a guard column (10 m × 2.1 mm, 3 μm particle). The mobile phase flow rate was 300 μL/min and the column temperature was maintained at 25 °C. The solvent system was 10 mM ammonium acetate (A) and acetonitrile (B), with the elution started isocratically at 0% B for 2 min, followed by a linear gradient from 0 to 12% B over 8 min and further to 40% B over 2.5 min, and finally the column was re-equilibrated at 0% B for 8 min. MS Operating parameters were as follows: ESI capillary voltage, 3000 V; gas temperature, 340 °C; drying gas flow, 10 L/min; nebulizer pressure, 20 psi; fragmentor voltage, 120 V; collision energy, 10eV. Samples were analyzed in multiple reaction monitoring mode, with the following transitions: *m/z* 284.1 → 168.1 and 253.1 → 137 for 8-oxodG and 2'-deoxyinosine (dI, internal standard), respectively. Calibration curves for the 8-oxodG were constructed by plotting the MRM signal ratios between the 8-oxodG and dI against their corresponding concentration ratios.

## RESULTS

In this study, we assessed the effect of local DNA sequence context on the reactivity of 8-oxodG-containing oligodeoxyribonucleotides toward oxidation by two oxidants, $ONOOCO_2^-$ and riboflavin-mediated photooxidation. The model oligodeoxyribonucleotide targets, which contained 8-oxodG in different three-nucleotide contexts (Table 1), were of a length that optimized the stability of the duplex forms and the need for sufficient mass spectrometric sensitivity and mass accuracy for quantification of the loss of the 8-oxodG-containing strand. The specific sequences, which represent a subset of all 16 possible trinucleotide G sequence contexts, cover the range of sequence-dependent G IP[5] and the range of reactivities toward oxidation by both $ONOOCO_2^-$ and riboflavin-mediated photooxidation observed previously.[9,10,19] AGC and TGC have the highest G IPs, CGA and CGT have intermediate IPs, and AGG and GGG have the lowest IPs. The reactivity of the central G in each trinucleotide sequence with $ONOOCO_2^-$ and riboflavin was directly and inversely correlated with IP, respectively.[9,10,19] To ensure that the oligodeoxyribonucleotides were stable in double-stranded DNA form during oxidation reactions, we used two different methods to establish that all six oligodeoxyribonucleotide substrates possessed melting temperatures in the range of 43–52 °C (Table 1), with experiments performed at 4–18 °C.

### Development of LC-MS methods for quantifying the reactivity of 8-oxodG-containing oligodeoxyribonucleotides

To quantify the reactivity of 8-oxodG-containing oligodeoxyribonucleotides toward oxidation and to locate the damage arising from 8-oxodG oxidation, we developed a liquid chromatography-coupled QTOF mass spectrometric method (LC-QTOF) to monitor changes in the quantity of each strand of the duplex oligodeoxyribonucleotide following oxidation reactions. The high mass accuracy of the QTOF system (<10 ppm) allowed us to uniquely identify the two strands. This is illustrated in Fig. 1 for the duplex oligodeoxyribonucleotide containing 8-oxodG in the GOG sequence context (Table 1; “O” denotes 8-oxodG). The extracted ion chromatogram in Fig. 1a shows complete resolution of the two strands of the oligodeoxyribonucleotide duplex and the internal standard, 5'-GATCTCGATC-3'. The oligodeoxyribonucleotides ionized most abundantly as triply-charged anions (data not shown) that produced a relatively well resolved isotopic envelope as shown in the mass spectrum in Fig. 1b, with the monoisotopic mass of the triply-charged GOG-containing oligodeoxyribonucleotide (*m/z* 1024.5092) differing by <5 ppm from the calculated *m/z* value (1024.5106). Relative quantification of each oligodeoxyribonucleotide was achieved by first normalizing the peak area for each molecular ion against that of the internal

NIH-PA Author Manuscript

NIH-PA Author Manuscript

NIH-PA Author Manuscript

standard, to account for variation in injection volume, followed by dividing the normalized peak area of the unreacted oligodeoxyribonucleotide in the treated sample by that in the untreated sample. This is illustrated in Fig. 1c for the reaction of the GOG- and GGG-containing oligodeoxyribonucleotides with a range of $ONOOCO_2^-$ concentrations. The greater reactivity of GOG compared to GGG shown in Fig. 1c is consistent with published studies demonstrating the greater reactivity of 8-oxodG toward oxidation[13,14] and provides validation of the LC-QTOF method for quantification of the relative reactivity of 8-oxodG in different sequence contexts.

To cross-validate our LC-QTOF-based quantification approach, we also developed a sensitive tandem QQQ method to quantify 8-oxodG-containing oligodeoxyribonucleotides. First, we performed collision-induced dissociation (CID) experiments on the oligodeoxyribonucleotides using high mass-accuracy QTOF mass spectrometry to define signature 8-oxodG-containing fragment ions. Fig. 1e shows the fragment ion ladder observed in LC-QTOF analysis of $[M-3H]^{3-}$ precursor of GOG oligodeoxyribonucleotide, which revealed abundant fragment ions with *m/z* 798.625 and 595.101 (Fig. S1). These fragment ions, which confirm the sequence location of the 8-oxodG moiety in GOG, correspond to the $W_5^{2-}$ fragment (GOGCC) and the $W_2^-$ fragment (CC), respectively (Fig. 1e). Then, a QQQ MRM method was used to quantify the signature fragment ions in oligodeoxyribonucleotides before and after treatment with oxidants. The LC-QQQ MRM results (Fig. 1d) were very similar to those obtained by LC-QTOF analysis of intact oligodeoxyribonucleotides (Fig. 1c).

A third approach involves a direct quantification of 8-oxodG as a 2'-deoxynucleoside following enzymatic hydrolysis of the oxidized oligodeoxyribonucleotides.[18] This approach provides the most sensitive analysis of 8-oxodG disappearance during the oxidation reactions and was used to corroborate the results obtained with analysis of the intact oligodeoxyribonucleotides (Fig. 2c & 4c).

### 8-oxodG reactivity with $ONOOCO_2^-$ and irradiated riboflavin

To examine the effect of sequence context on the oxidation of 8-oxodG, we quantified the loss of the parent 8-oxodG-containing strand of the duplex oligodeoxyribonucleotides (Table 1) treated with a range of concentrations of $ONOOCO_2^-$. As shown in the dose-response curves in Fig. 2a, there is no significant sequence-dependence for the reactivity of 8-oxodG with $ONOOCO_2^-$ over a three order-of-magnitude concentration range (2.5 μM-2 mM). At $ONOOCO_2^-$ concentrations from 0.2 to 2 mM, more than 30% of each 8-oxodG-containing oligodeoxyribonucleotide was consumed, which, by Poisson statistics, indicates multiple damage events in each oligodeoxyribonucleotide.[10] Even under “single-hit” conditions (i.e., 2.5 – 200 μM), in which damage occurred in <30% of the parent oligodeoxyribonucleotides, we did not observe any major effect of local sequence on 8-oxodG reactivity with $ONOOCO_2^-$ (Fig. 2b). This is demonstrated quantitatively in Fig. 3a through comparison of areas under curves (AUC) for the different sequences in the abundance versus $ONOOCO_2^-$ concentration plot (Fig. 2a), revealing only a single statistically significant difference between GOG and COT (Fig. 3a).

Further corroboration of the lack of sequence effects on 8-oxodG oxidation by $ONOOCO_2^-$ was obtained by the direct LC-MS/MS quantification of 8-oxodG in $ONOOCO_2^-$-treated AOC and AOG, which represent the most and least reactive sequence contexts for G oxidation, respectively.[10] As shown in Fig. 2c and Fig. S2a, there was no significant difference in the levels of 8-oxodG in the two oligodeoxyribonucleotides. These experiments point to minimal sequence context effects on the oxidation of 8-oxodG by $ONOOCO_2^-$, which stands in contrast to the striking sequence-dependence of G oxidation by $ONOOCO_2^-$ observed previously.[10]

NIH-PA Author Manuscript

NIH-PA Author Manuscript

NIH-PA Author Manuscript

We also performed similar LC-QTOF studies for riboflavin-mediated photooxidation of 8-oxodG in different sequence contexts. Control reactions with either UV or riboflavin exposure in the absence of light showed the expected minimal loss of 8-oxodG (Fig. S3). Fig. S3 also confirmed that 8-oxodG, and not other Gs in the oligodeoxyribonucleotide substrates, was the target for riboflavin-mediated photooxidation, as indicated by the lack of reaction of oligodeoxyribonucleotides containing G under the conditions that produced significant oxidation of 8-oxodG. The photoactivation of riboflavin produced significant oxidation of 8-oxodG that, unlike $ONOOCO_2^-$, varied significantly as a function of sequence context, across a range of concentrations up to 90 μM riboflavin (Fig. 4a). The LC-MS/MS MRM results (Fig. 4b) were identical to those obtained by LC-QTOF analysis of intact oligodeoxyribonucleotides (Fig. 4a).

Further, the direct LC-MS/MS quantification of 8-oxodG in the AOC and AOG oligodeoxyribonucleotides revealed significantly greater reactivity of 8-oxodG in the AOG context (Fig. 4c & S2b), in contrast to lack of effect observed with $ONOOCO_2^-$ (Fig. 2c). As shown in Fig. 3b, a comparison of reactivity data (Fig. 4a) reveals statistically significant differences between most of the sequence contexts for riboflavin-mediated photooxidation.

## DISCUSSION

To define the role of sequence context in the reactivity of 8-oxodG toward oxidation, we employed an oligodeoxyribonucleotide-based high-resolution mass spectrometry approach that is less labor intensive, offers higher throughput and is more precise than previous methods based on polyacrylamide gel electrophoresis (e.g., refs. 10,17,19,20), as well as offering the potential for identifying individual damage products in other applications. Control experiments verified that the oligodeoxyribonucleotide substrates were fully in the duplex form and that 8-oxodG was the primary target for oxidation in the site-specifically labeled oligodeoxyribonucleotides.

Our findings indicate that the reactivity of 8-oxodG toward oxidation not only depends upon local sequence context but also upon the oxidant. Unlike riboflavin-mediated photooxidation, 8-oxodG oxidation by $ONOOCO_2^-$ showed little if any sequence dependence. This stands in contrast to our earlier report on sequence-dependent dG oxidation by $ONOOCO_2^-$, where CGC, AGC and TGC were found to be highly reactive,[10,11] and to evidence from a limited number of studies showing heightened reactivity of 8-oxodG when it is positioned 5' to a dG than when located in a 3' position.[13,17] On the basis of our earlier studies,[10,19,21,22] we propose that this lack of sequence dependence for $ONOOCO_2^-$ oxidation of 8-oxodG reflects the simultaneous generation of two oxidants (i.e., $^{\bullet}NO_2$ and $CO_3^{\bullet-}$) and the influence of hole migration from the sites of initial electron removal from G residues within the duplex to 8-oxoG and the rate of final product formation. Both $CO_3^{\bullet-}$ and $^{\bullet}NO_2$, with their reduction potentials of 1.59 and 1.04 V versus NHE, respectively,22–25 are capable of oxidizing 8-oxodG ($E^0$ = 0.74 V versus NHE[16]) to form the 8-oxodG radical cation (8-oxodG$^{\bullet+}$) (Scheme 1). While $CO_3^{\bullet-}$ can also oxidize dG ($E^0$ = 1.29 V versus NHE[15]) in the oligodeoxyribonucleotide substrates, our results demonstrate that initial oxidation of 8-oxodG by $CO_3^{\bullet-}$ or $^{\bullet}NO_2$ dominates the generation of end-products in these oligodeoxyribonucleotides, which is likely due to the significantly greater reactivity of 8-oxodG compared to G. Once formed, the 8-oxodG$^{\bullet+}$ can be trapped by further oxidation or by reactions with species such as superoxide (Scheme 1), and it is thus possible that the combined activity of two oxidizing radical species ($CO_3^{\bullet-}$ or $^{\bullet}NO_2$) masks whatever differences there are in sequence-dependent reactivity of 8-oxodG or stability of the resulting 8-oxodG$^{\bullet+}$. In this model, either radical can perform the initial electron removal to form 8-oxodG$^{\bullet+}$, with the remaining radical or other local reactive species, such as superoxide, quickly oxidizing or trapping the radical cation. Since oxidation

NIH-PA Author Manuscript

NIH-PA Author Manuscript

NIH-PA Author Manuscript

of 8-oxodG by $^{\bullet}NO_2$ is kinetically slower than that by $CO_3^{\bullet-}$ by a factor of ~60,[21,22,26,27] it is possible that $CO_3^{\bullet-}$ will be more competitive for the initial 8-oxodG oxidation and that $^{\bullet}NO_2$ will perform the subsequent oxidation. Thus, the presence of two oxidants may account for the lack of sequence selectivity in reactions of $ONOOCO_2^-$ with 8-oxodG in DNA.

The observed lack of sequence context effects on 8-oxodG oxidation by $ONOOCO_2^-$ differs dramatically from the strong effect of surrounding nucleobases on the oxidation of dG.[10] The lower reactivity of dG toward oxidation and the inability of $^{\bullet}NO_2$ to oxidize dG may increase the probability of hole migration from an initially formed G radical cation and thus account for the different sequence context effects for oxidation of dG and 8-oxodG by $ONOOCO_2^-$. The extent to which local sequence context affects electron removal from 8-oxodG relative to G may also account for the observed differences in reactivity toward $ONOOCO_2^-$, but data are lacking on the possible sequence-dependent differences in 8-oxodG ionization potential.

In contrast to $ONOOCO_2^-$, the reactivity of 8-oxodG towards riboflavin-mediated photooxidation varied widely for different sequence contexts: COA ≈ AOG > GOG > COT > TOC > AOC. The major oxidizing species generated by UVA-irradiated riboflavin are triplet state riboflavin radicals with some generation of singlet oxygen.[28] On the basis of studies with G oxidation, 8-oxodG oxidation by photoactivated riboflavin can be either direct or indirect. The direct mechanism involves electron transfer from 8-oxodG to triplet riboflavin to form the 8-oxodG radical cation, with the riboflavin radical anion reducing oxygen to superoxide. The indirect mechanism can occur by initial electron transfer from riboflavin triplet to $O_2$ to form riboflavin radical cation and superoxide, with the riboflavin radical cation oxidizing 8-oxodG (Scheme 1).[29] By either mechanism, the resulting spectrum of products consists primarily of Iz, DGh, Gh and Sp (Scheme 1; refs. 30–34). One model to explain the sequence-selective oxidation of 8-oxodG by photoactivated riboflavin parallels that proposed for G oxidation by sulfate radical ($SO_4^{\bullet-}$).[35] Both triplet riboflavin and $SO_4^{\bullet-}$ are strong oxidants (1.7 V and 2.4 V versus NHE, respectively; refs. 24,36) with the ability to remove electrons relatively indiscriminately from all four nucleobases.[15] The resulting hole then migrates to the site with the lowest IP, which would be 8-oxodG, with 8-oxodG reactivity modulated by sequence-dependent variations in the IP of 8-oxodG and neighboring bases. This model is supported by the limited number of studies of sequence-dependence of 8-oxodG oxidation done to date,[13,17] which reveal that 8-oxodG is more reactive with a variety of one-electron oxidants and it has a lower IP when positioned 5' to a G than when located in a 3' position. This parallels G reactivity with riboflavin-mediated photooxidation (e.g., ref. 19). However, while there are some similarities in the sequence-dependence of G and 8-oxodG reactivity toward oxidation, there are important differences, most notably that photoactivated riboflavin favors COA and AOG over GOG. If sequence-dependent IP governs 8-oxodG oxidation as it does with G oxidation, then the sequence-dependent IP values for 8-oxodG must differ from those of G, which fall in increasing IP as follows: GGG > AGG > CGA > CGT > AGC > TGC.[9,10] Further studies are needed to define 8-oxodG IP values in all possible sequence contexts.

Analysis of G oxidation chemistry and the mutations caused by riboflavin-mediated photooxidation of G yields some insights into the sequence-dependent differences in 8-oxodG reactivity observed here. Studies with site-specifically positioned 8-oxodG and with *E. coli* lacking formamidopyrimidine-DNA glycosylase (Fpg) have revealed that hotspots for 8-oxodG mutations, which are almost exclusively G:C to T:A, occur in a consensus sequence of 5'-PuOPu-3' (where O = 8-oxodG; refs. 37–41). However, in addition to G:C to T:A, riboflavin-mediated photooxidation of DNA results in a significant number of G:C to A:T and G:C to C:G mutations (Table S2).39–41 Further, while polymerase-mediated effects on the mutation spectrum must be taken into account, these mutations occur at high

NIH-PA Author Manuscript

NIH-PA Author Manuscript

NIH-PA Author Manuscript

frequency in sequence contexts that we observed to be highly reactive with photoactivated riboflavin (COA, GOG; Table S2). The G:C to A:T and G:C to C:G mutations cannot be explained by 8-oxodG, which suggests that other damage products are produced during G oxidation, such as 8-oxodG oxidation products. This is supported by the observations of Schulz et al. that Fpg-sensitive lesions (e.g., 8-oxodG, FapyG) accounted for a minority of damage products caused by photoactivated riboflavin oxidation of G.[41] Interestingly, Takimoto et al. observed that the formation of the riboflavin-induced G oxidation products giving rise to G:C to C:G mutations was kinetically slow, over several hours.[39] This is consistent with the slow kinetics of degradation of the 8-oxodG oxidation products DGh, which converts to OA with a half-life of ~5 hr[42] and then to UA with a half-life of ~40 hr,[43] and Iz, which undergoes hydrolysis to Ox with a half-life of ~2.5 hr[44] (Scheme 1).

While these models await verification of the effects of sequence context on the spectrum of G and 8-oxodG damage products, the observation of the sequence- and oxidant-dependence of 8-oxodG oxidation raise important questions about the effects of the heightened reactivity of 8-oxodG relative to G on the ultimate biological endpoint of mutation.

## Supplementary Material

Refer to Web version on PubMed Central for supplementary material.

## Acknowledgments

**FUNDING SOURCES** Mass spectrometry studies were performed in the Bioanalytical Facilities Core of the MIT Center for Environmental Health Sciences, which is funded by Center Grant ES002109 from the National Institute of Environmental Health Sciences. This work was also supported by grants from the National Cancer Institute (CA026731 and CA110261).

The authors thank Ms. Jia Ling Siau for discussion related to peroxynitrite, Dr. Shuguang Zhang and Karolina A. Corin of the MIT Center for Biomedical Engineering for assistance with circular dichroism studies.

## The abbreviations used are

| | |
|---|---|
| **8-oxodG** | 8-oxo-7,8-dihydro-2'-deoxyguanosine |
| **CD** | circular dichroism |
| **CID** | collision-induced dissociation |
| **ESI** | electrospray ionization |
| **LC** | liquid chromatography |
| **MRM** | multiple reaction monitoring |
| **MS** | mass spectrometry |
| **QQQ** | triple quadrupole |
| **QTOF** | quadrupole time-of-flight |

## REFERENCES

(1). Budowsky EI, Kovalsky OI, Yakovlev D, Simukova NA, Rubin LB. Footprinting of DNA secondary structure by high-intensity (laser) ultraviolet irradiation. FEBS Lett. 1985; 188:155–158. [PubMed: 4018270]

(2). Giese B. Electron transfer in DNA. Curr. Opin. Chem. Biol. 2002; 6:612–618. [PubMed: 12413545]

NIH-PA Author Manuscript

NIH-PA Author Manuscript

NIH-PA Author Manuscript

(3). Schuster GB. Long-range charge transfer in DNA: transient structural distortions control the distance dependence. Acc. Chem. Res. 2000; 33:253–260. [PubMed: 10775318]

(4). Ito K, Inoue S, Yamamoto K, Kawanishi S. 8-Hydroxydeoxyguanosine formation at the 5' site of 5'-GG-3' sequences in double-stranded DNA by UV radiation with riboflavin. J. Biol. Chem. 1993; 268:13221–13227. [PubMed: 8390459]

(5). Sugiyama H, Saito I. Theoretical studies of GG-specific photocleavage of DNA via electron transfer: significant lowering of ionization potential and 5'-localization of HOMO of stacked GG bases in B-form DNA. J. Am. Chem. Soc. 1996; 118:7063–7068.

(6). Saito I, Takayama M, Sugiyama H, Nakatani K. Photoinduced DNA cleavage via electron transfer: Demonstration that guanine residues located 5'- to a guanine are the most electron-donating sites. J. Am. Chem. Soc. 1995; 117:6406–6407.

(7). Senthilkumar K, Grozema FC, Guerra CF, Bickelhaupt FM, Siebbeles LDA. Mapping the sites of selective oxidation of guanines in DNA. J. Am. Chem. Soc. 2003; 125:13658–13659. [PubMed: 14599193]

(8). Cadet J, Douki T, Ravanat JL, Di Mascio P. Sensitized formation of oxidatively generated damage to cellular DNA by UVA radiation. Photochem. Photobiol. Sci. 2009; 8:903–911. [PubMed: 19582264]

(9). Saito I, Nakamura T, Nakatani K, Yoshioka Y, Yamaguchi K, Sugiyama H. Mapping of the hot spots for DNA damage by one-electron oxidation: Efficacy of GG doublets and GGG triplets as a trap in long-range hole migration. J. Am. Chem. Soc. 1998; 120:12686–12687.

(10). Margolin Y, Cloutier JF, Shafirovich V, Geacintov NE, Dedon PC. Paradoxical hotspots for guanine oxidation by a chemical mediator of inflammation. Nat. Chem. Biol. 2006; 2:365–366. [PubMed: 16751762]

(11). Lee YA, Durandin A, Dedon PC, Geacintov NE, Shafirovich V. Oxidation of guanine in G, GG, and GGG sequence contexts by aromatic pyrenyl radical cations and carbonate radical anions: relationship between kinetics and distribution of alkali-labile lesions. J. Phys. Chem. B. 2008; 112:1834–1844. [PubMed: 18211057]

(12). Dedon PC, Tannenbaum SR. Reactive nitrogen species in the chemical biology of inflammation. Arch. Biochem. Biophys. 2004; 423:12–22. [PubMed: 14989259]

(13). Sheu C, Foote CS. Reactivity toward singlet oxygen of a 7,8-dihydro-8-oxoguanosine (“8-hydroxyguanosine”) formed by photooxidation of a guanosine derivative. J. Am. Chem. Soc. 1995; 117:6439–6442.

(14). Uppu RM, Cueto R, Squadrito GL, Salgo MG, Pryor WA. Competitive reactions of peroxynitrite with 2'-deoxyguanosine and 7,8-dihydro-8-oxo-2'-deoxyguanosine (8-oxodG): Relevance to the formation of 8-oxodG in DNA exposed to peroxynitrite. Free Rad. Biol. Med. 1996; 21:407–411. [PubMed: 8855454]

(15). Steenken S, Jovanovic SV. How easily oxidizable is DNA? One-electron reduction potentials of adenosine and guanosine radicals in aqueous solution. J. Am. Chem. Soc. 1997; 119:617–618.

(16). Steenken S, Jovanovic SV, Bietti M, Bernhard K. The trap depth (in DNA) of 8-oxo-7,8-dihydro-2'-deoxyguanosine as derived from electron-transfer equilibria in aqueous solution. J. Am. Chem. Soc. 2000; 122:2373–2374.

(17). Hickerson RP, Prat F, Muller JG, Foote CS, Burrows CJ. Sequence and stacking dependence of 8-oxoguanine oxidation: Comparison of one-electron vs singlet oxygen mechanisms. J. Am. Chem. Soc. 1999; 121:9423–9428.

(18). Taghizadeh K, McFaline JL, Pang B, Sullivan M, Dong M, Plummer E, Dedon PC. Quantification of DNA damage products resulting from deamination, oxidation and reaction with products of lipid peroxidation by liquid chromatography isotope dilution tandem mass spectrometry. Nat. Protoc. 2008; 3:1287–1298. [PubMed: 18714297]

(19). Margolin Y, Shafirovich V, Geacintov NE, DeMott MS, Dedon PC. DNA sequence context as a determinant of the quantity and chemistry of guanine oxidation produced by hydroxyl radicals and one-electron oxidants. J. Biol. Chem. 2008; 283:35569–35578. [PubMed: 18948263]

(20). Tretyakova NY, Burney S, Pamir B, Wishnok JS, Dedon PC, Wogan GN, Tannenbaum SR. Peroxynitrite-induced DNA damage in the *supF* gene: correlation with the mutational spectrum. Mutat. Res. 2000; 447:287–303. [PubMed: 10751613]

NIH-PA Author Manuscript

NIH-PA Author Manuscript

NIH-PA Author Manuscript

(21). Lee YA, Yun BH, Kim SK, Margolin Y, Dedon PC, Geacintov NE, Shafirovich V. Mechanisms of oxidation of guanine in DNA by carbonate radical anion, a decomposition product of nitrosoperoxycarbonate. Chemistry. 2007; 13:4571–4581. [PubMed: 17335089]

(22). Shafirovich V, Dourandin A, Huang W, Geacintov NE. The carbonate radical is a site-selective oxidizing agent of guanine in double-stranded oligonucleotides. J. Biol. Chem. 2001; 276:24621–24626. [PubMed: 11320091]

(23). Stanbury DM. Reduction potentials involving inorganic free radicals in aqueous solution. Adv. Inorg. Chem. 1989; 33:69–138.

(24). Huie RE, Clifton CL, Neta P. Electron transfer reaction rates and equilibria of the carbonate and sulfate radical anions. Radiat. Phys. Chem. 1991; 38:477–481.

(25). Buettner GR. The pecking order of free radicals and antioxidants: lipid peroxidation, alpha-tocopherol, and ascorbate. Arch Biochem Biophys. 1993; 300:535–543. [PubMed: 8434935]

(26). Shafirovich V, Cadet J, Gasparutto D, Dourandin A, Geacintov NE. Nitrogen dioxide as an oxidizing agent of 8-oxo-7,8-dihydro-2'-deoxyguanosine but not of 2'-deoxyguanosine. Chem. Res. Toxicol. 2001; 14:233–241. [PubMed: 11258973]

(27). Joffe A, Mock S, Yun BH, Kolbanovskiy A, Geacintov NE, Shafirovich V. Oxidative generation of guanine radicals by carbonate radicals and their reactions with nitrogen dioxide to form site specific 5-guanidino-4-nitroimidazole lesions in oligodeoxynucleotides. Chem. Res. Toxicol. 2003; 16:966–973. [PubMed: 12924924]

(28). Hiraku Y, Ito K, Hirakawa K, Kawanishi S. Photosensitized DNA damage and its protection via a novel mechanism. Photochem. Photobiol. 2007; 83:205–212. [PubMed: 16965181]

(29). Lu C, Lin W, Wang W, Han Z, Yao S, Lin N. Riboflavin (VB2) photosensitized oxidation of 2'-deoxyguanosine-5'-monophosphate (dGMP) in aqueous solution: a transient intermediates study. Phys. Chem. Chem. Phys. 2000; 2:329–334.

(30). Spassky A, Angelov D. Influence of the local helical conformation on the guanine modifications generated from one-electron DNA oxidation. Biochemistry. 1997; 36:6571–6576. [PubMed: 9184136]

(31). Leipold MD, Muller JG, Burrows CJ, David SS. Removal of hydantoin products of 8-oxoguanine oxidation by the Escherichia coli DNA repair enzyme, FPG. Biochemistry. 2000; 39:14984–14992. [PubMed: 11101315]

(32). Douki T, Cadet J. Modification of DNA bases by photosensitized one-electron oxidation. Internat. J. Rad. Biol. 1999; 75:571–581.

(33). Kino K, Sugiyama H. Possible cause of G-C-->C-G transversion mutation by guanine oxidation product, imidazolone. Chem. Biol. 2001; 8:369–378. [PubMed: 11325592]

(34). Haraguchi K, Delaney MO, Wiederholt CJ, Sambandam A, Hantosi Z, Greenberg MM. Synthesis and characterization of oligodeoxynucleotides containing formamidopyrimidine lesions and nonhydrolyzable analogues. J. Am. Chem. Soc. 2002; 124:3263–3269. [PubMed: 11916409]

(35). Lee YA, Liu Z, Dedon PC, Geacintov NE, Shafirovich V. Solvent Exposure Associated with Single Abasic Sites Alters the Base Sequence Dependence of Oxidation of Guanine in DNA in GG Sequence Contexts. Chembiochem. 2011; 12:1731–1739. [PubMed: 21656632]

(36). Yoshimura A, Ohno T. Lumiflavin-sensitized photooxygenation of indole. Photochem. Photobiol. 1988; 48:561–565. [PubMed: 3241828]

(37). Hatahet Z, Zhou M, Reha-Krantz LJ, Morrical SW, Wallace SS. In search of a mutational hotspot. Proc. Natl. Acad. Sci. USA. 1998; 95:8556–8561. [PubMed: 9671716]

(38). Watanabe T, Nunoshiba T, Kawata M, Yamamoto K. An in vivo approach to identifying sequence context of 8-oxoguanine mutagenesis. Biochem. Biophys. Res. Commun. 2001; 284:179–184. [PubMed: 11374888]

(39). Takimoto K, Tano K, Hashimoto M, Hori M, Akasaka S, Utsumi H. Delayed transfection of DNA after riboflavin mediated photosensitization increases G:C to C:G transversions of *supF* gene in *Escherichia coli* mutY strain. Mutat. Res. 1999; 445:93–98. [PubMed: 10521694]

(40). Besaratinia A, Kim SI, Bates SE, Pfeifer GP. Riboflavin activated by ultraviolet A1 irradiation induces oxidative DNA damage-mediated mutations inhibited by vitamin C. Proc. Natl. Acad. Sci. USA. 2007; 104:5953–5958. [PubMed: 17389394]

NIH-PA Author Manuscript

NIH-PA Author Manuscript

NIH-PA Author Manuscript

(41). Schulz I, Mahler HC, Boiteux S, Epe B. Oxidative DNA base damage induced by singlet oxygen and photosensitization: recognition by repair endonucleases and mutagenicity. Mutat. Res. 2000; 461:145–156. [PubMed: 11018587]

(42). Chworos A, Seguy C, Pratviel G, Meunier B. Characterization of the dehydro-guanidinohydantoin oxidation product of guanine in a dinucleotide. Chem. Res. Toxicol. 2002; 15:1643–1651. [PubMed: 12482248]

(43). Henderson PT, Neeley WL, Delaney JC, Gu F, Niles JC, Hah SS, Tannenbaum SR, Essigmann JM. Urea lesion formation in DNA as a consequence of 7,8-dihydro-8-oxoguanine oxidation and hydrolysis provides a potent source of point mutations. Chem. Res. Toxicol. 2005; 18:12–18. [PubMed: 15651843]

(44). Duarte V, Gasparutto D, Jaquinod M, Cadet J. In vitro DNA synthesis opposite oxazolone and repair of this DNA damage using modified oligonucleotides. Nucleic Acids Res. 2000; 28:1555–1563. [PubMed: 10710422]

NIH-PA Author Manuscript

NIH-PA Author Manuscript

NIH-PA Author Manuscript

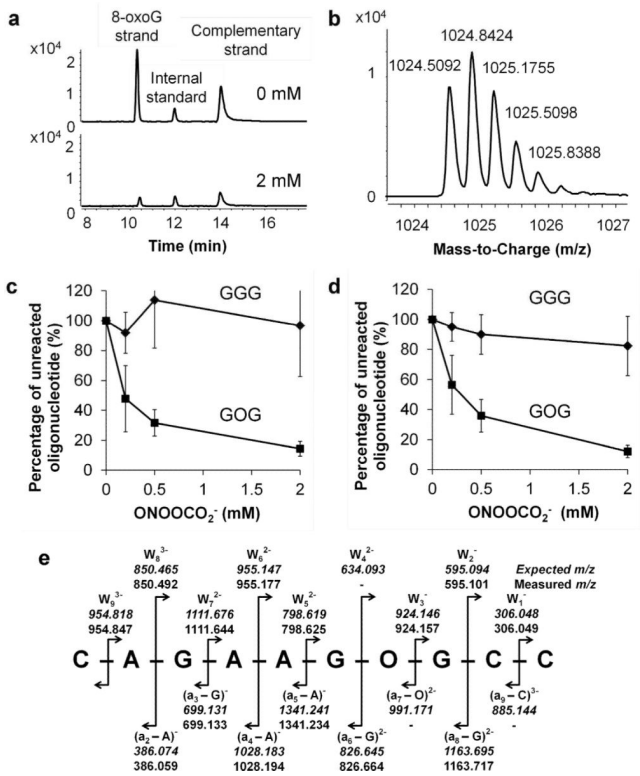


**Figure 1.**

LC-QTOF analysis of 8-oxodG-containing duplex oligodeoxyribonucleotides. (a) Extracted ion chromatograms of the GOG oligodeoxyribonucleotide duplex before (upper) and after (lower) treatment with 2 mM $ONOOCO_2^-$. GATCTCGATC internal standard was added after treatment. (b) TOF mass spectrum of the triply-charged GOG oligodeoxyribonucleotide showing a monoisotopic *m/z* value of 1024.50920 and a well resolved isotopic envelope. (c, d) Scatter plots showing results from (c) QTOF and (d) QQQ analysis of the relative reactivity of $ONOOCO_2^-$ with oligodeoxyribonucleotide duplexes containing either GGG or GOG sequence contexts. (e) Illustration of CID localization of 8-oxodG in the GOG oligodeoxyribonucleotide, with expected (in italics, upper row) and measured (lower row) *m/z* values.

NIH-PA Author Manuscript

NIH-PA Author Manuscript

NIH-PA Author Manuscript

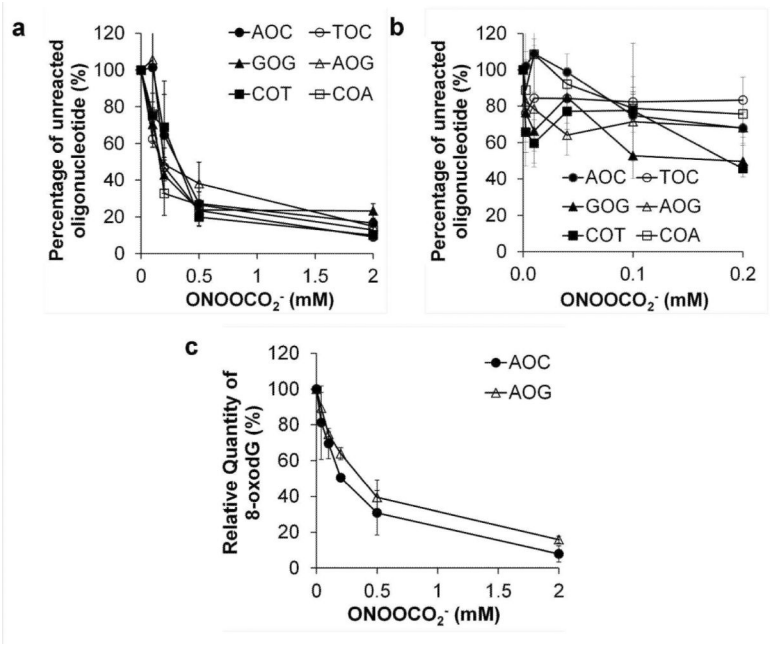


**Figure 2.**

Reactivity of 8-oxodG-containing oligodeoxyribonucleotides with $ONOOCO_2^-$. (a,b) LCQTOF analysis of duplex oligodeoxyribonucleotides were treated with (a) 0, 0.1, 0.2, 0.5, or 2 mM $ONOOCO_2^-$, or (b) 0, 0.0025, 0.05, 0.1 or 0.2 mM $ONOOCO_2^-$. Each data point represents mean ± SD of three independent experiments, with Student's T-test at $P<0.05$ revealing no significant differences in reactivity. (c) Direct analysis of 8-oxodG in AOC and AOG oligodeoxyribonucleotides treated with varying concentrations of $ONOOCO_2^-$. The oligodeoxyribonucleotides were digested to 2'-deoxyribonucleosides before LC-QQQ quantification of 8-oxodG. Each data point represents an average of two separate samples.

NIH-PA Author Manuscript

NIH-PA Author Manuscript

NIH-PA Author Manuscript

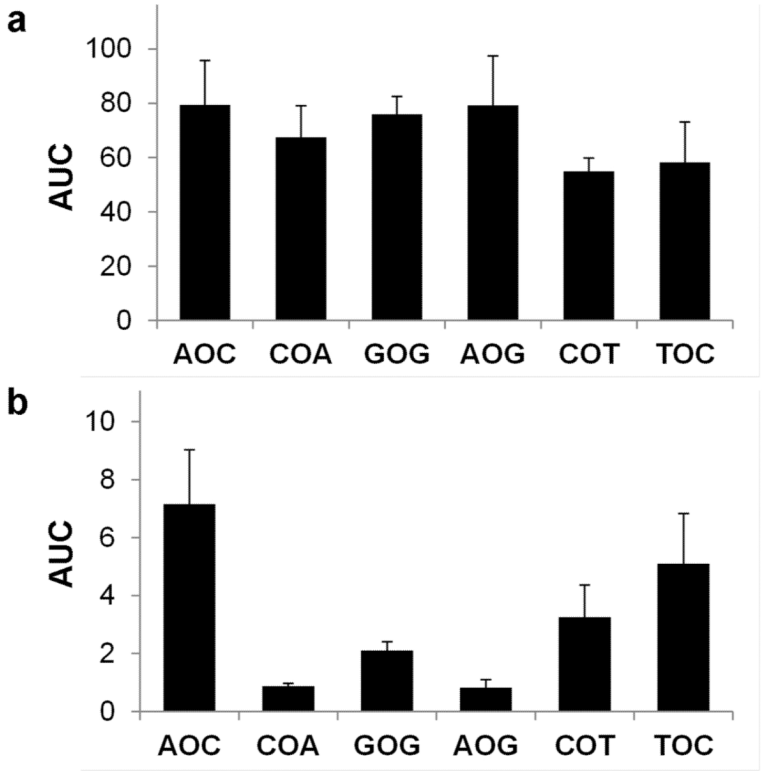


**Figure 3.**

Comparison of sequence-dependent reactivity of 8-oxodG with $ONOOCO_2^-$ and photoactivated riboflavin. Loss of oligodeoxyribonucleotides containing 8-oxodG in different sequence contexts following oxidation with either (a) $ONOOCO_2^-$ or (b) photoactivated riboflavin was quantified as the area under the curve (AUC) values for the dose-response graphs in Figures 2A and 4A. AUC values were calculated by the trapezoidal method for each replicate data set, with mean and standard deviation calculated for 3 independent experiments. The lower the AUC value the higher the reactivity. Correlation analysis of $ONOOCO_2^-$ and riboflavin reactivity dose-response curves revealed significant differences ($P < 0.05$ by Student's t-test) for pair-wise comparisons of AUC values for 8-oxodG sequence contexts (abbreviations in Table 1). For $ONOOCO_2^-$, only GOG and COT were significantly different; for riboflavin-mediated photooxidation, all comparisons were significantly different except for COA vs. AOG, GOG vs. COT, AOC vs. TOC and COT vs. TOC.

NIH-PA Author Manuscript

NIH-PA Author Manuscript

NIH-PA Author Manuscript

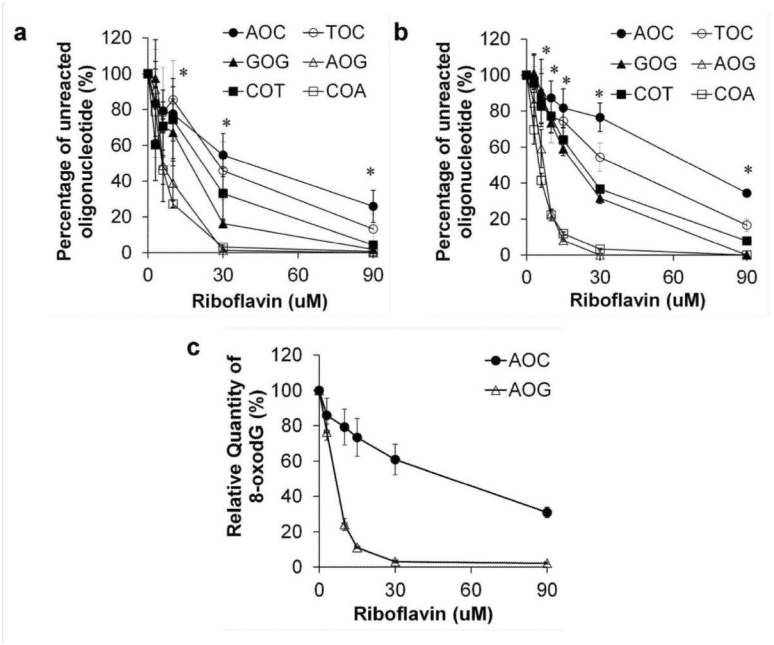


**Figure 4.**

Reactivity of 8-oxodG-containing oligodeoxyribonucleotides with photosensitized riboflavin. 8-oxodG-containing duplex oligodeoxyribonucleotides were treated with varying concentrations of riboflavin (0, 3, 6, 10, 30 and 90 μM) and a constant level of UVA irradiation at 4 °C for 20 min, as described in Materials and Methods. The oligodeoxyribonucleotides were then analyzed by (a) LCQTOF or (b) LC-QQQ. Each data point represents the mean ± S.D. of 3 samples; asterisks denote significant differences by ANOVA, $P < 0.01$. (c) Targeted quantification of 8-oxodG in AOC and AOG oligodeoxyribonucleotides treated with varying concentrations of photosensitized riboflavin (0–90 μM) and then digested to nucleosides for LC-QQQ analysis. Data represent mean ± error about the mean for analysis of two samples.

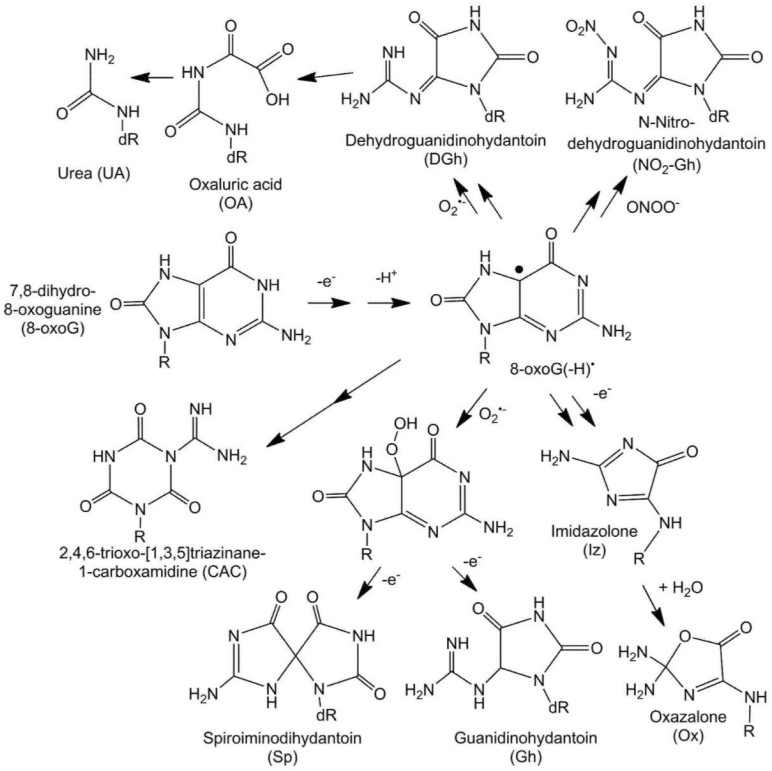


**Scheme 1.**

Mechanisms and products of 8-oxodG oxidation by photoactivated riboflavin and nitrosoperoxycarbonate.



NIH-PA Author Manuscript NIH-PA Author Manuscript NIH-PA Author Manuscript

NIH-PA Author Manuscript

NIH-PA Author Manuscript

NIH-PA Author Manuscript

## Table 1

Oligodeoxyribonucleotide constructs containing 8-oxodG in different sequence contexts[a].

| Name | 8-oxodG strand | Complementary strand | Tm (°C)[b] | G Ionization Potential, eV[c] |
|---|---|---|---|---|
| AOC | CAGAA**AOC**CC | GGGCTTTCTG | 49.8/49.5 | 7.01 |
| COA | CAGAA**COA**CC | GGTCGTTCTG | 46.2/44.2 | 6.63 |
| GOG | CAGAA**GOG**CC | GGCCCTTCTG | 43.6/50.1 | 6.44 |
| AOG | CAGAA**AOG**CC | GGCCTTTCTG | 48.2/51.3 | 6.5 |
| COT | CAGAA**COT**CC | GGACGTTCTG | 44.9/43.4 | 6.91 |
| TOC | CAGAA**TOC**CC | GGGCATTCTG | 45.7/47.1 | 7.12 |
| AGC | CAGAA**AGC**CC | GGGCTTTCTG | ND | - |
| CGA | CAGAA**CGA**CC | GGTCGTTCTG | ND | - |
| GGG | CAGAA**GGG**CC | GGCCCTTCTG | ND | - |

[a] The position of 8-oxodG is denoted by “O”.

[b] Melting temperature was determined by circular dichroism/real-time PCR; ND, not determined.

[c] Sequence-specific ionization potentials for G in the 3-nucleotide context noted for 8-oxodG, as calculated by Saito et al. in ref. 9.